# Imaging, Modelfitting, and Source Structure Corrections for the K-band (24 GHz) Celestial Reference Frame

A. de Witt, C. Jacobs, D. Gordon, M. Bietenholz, H. Krásná, M. Johnson, L. Hunt, N. Mwiya, M. Nickola

**Abstract** The K-band (24-GHz) celestial reference frame (K-CRF) program, supported through the United States Naval Observatory's (USNO) 50% timeshare allocation of the Very Long Baseline Array (VLBA), has so far provided high-resolution VLBA images for more than 800 Active Galactic Nuclei (AGN) at up to 81 epochs, as part of extending the International Celestial Reference Frame (ICRF) to K-band. A comprehensive analysis of these images has yielded metrics that serve as indicators for the suitability of each source as a calibrator or reference point. Additionally, our modelling efforts provide crucial insights into the overall dimensions and orientation of the source structure. Although AGN such as the Celestial Reference Frame (CRF) sources typically appear more compact at K-band than at X-band (8.4 GHz), they can, on occasion, still display noticeable extended emissions at K-band. We therefore initiated a project aimed at modelling structure effects in the astrometric analysis process. This involves utilizing readily available K-CRF VLBI images and up-to-date source structure models. This paper offers an overview of our image analysis efforts and outlines our plans to investigate the impact of source structure using all available K-CRF sources.

**Keywords** VLBI imaging, astrometry, celestial reference frame, AGN, K-band, 24 GHz

Aletha de Witt · Michael Bietenholz · Marisa Nickola
South African Radio Astronomy Observatory (SARAO), P.O. Box 443, Krugersdorp 1740, South Africa

Chistopher Jacobs
Jet Propulsion Laboratory (JPL), California Institute of Technology (CIT), 4800 Oak Grove Drive, Pasadena, CA 91109, USA

David Gordon · Megan Johnson
U.S. Naval Observatory (USNO), 3450 Massachusetts Ave NW, Washington, DC 20392, USA

Hana Krásná
Technische Universität Wien, Wiedner Hauptstraße 8-10/E120.4, Vienna, 1040, Austria

Lucas Hunt
National Radio Astronomy Observatory (NRAO), 800 Bradbury SE, Suite 235, Albuquerque, NM 87106, USA

Namakau Mwiya
University of Lusaka, P.O. Box 36711, Lusaka, Zambia

## 1 Imaging Status

The K-band celestial reference frame (K-CRF) program[1] has recently published high-resolution Very Long Baseline Interferometer (VLBI) images of 732 Active Galactic Nuclei (AGN) spanning up to 28 epochs per source, totalling an impressive 5078 images (de Witt et al., 2023b). All these images have been derived exclusively from monthly/bi-monthly 24-hour Very Long Baseline Array (VLBA, Napier, 1995) sessions observed from July 2015 to July 2018. The sessions were all observed in right circular polarization (RCP) using a data rate of 2 Gbps. Approximately 250 sources were observed in each session.

Building on this achievement, we have further expanded our imaging efforts by completing imaging for an additional 5 VLBA sessions observed from September 2018 to November 2018. As a result, we have now successfully captured images of 817 sources at up to 33 epochs, resulting in a total of 6095 images (available from our K-band imaging database[2]).

[1] K-band AstroGeo VLBI Project webpage
[2] K-band Imaging Database

The imaging for observations between December 2018 and January 2023 is completed and will be accessible in our database in December 2023, once modelfitting is finalized. This will increase the number of sources to more than 820 and will add 48 additional epochs (11 epochs at 2 Gbps RCP and 37 epochs at 4 Gbps dual-polarization), totalling 81 epochs. The imaging process for all VLBA sessions up to August 2023 is in its final stages and will result in a database of over 16,000 images.

## 2 Imaging, Analysis and Results

For imaging purposes, the correlated visibility data from our K-CRF VLBA observations are calibrated using the NRAO's Astronomical Imaging Processing System (AIPS, Greisen, 2003) via a semi-automated approach. The data calibration largely follows the VLBA calibration pipeline, utilizing standard AIPS utilities. An automated pipeline is employed for self-calibration, imaging, and deconvolution with the Caltech Difference Mapping software (DIFMAP, Shepherd, 1997). Custom Python routines generate images, $u, v$-coverage plots, and scan-averaged calibrated visibility amplitude plots. For example, such plots for the source NRAO140 (J0336+3218) from our K-CRF VLBA observations on 27 Oct 2018, are shown in Figure 1.

From each final K-band image, we extract various image parameters, including the peak brightness, total CLEAN flux density and the weighted average correlated flux density for four baseline length ranges (as shown in Figure 2), the background rms brightness level over the entire residual image and the image signal-to-noise-ratio (SNR), the quality of the fit between the observed and model visibilities after self-calibration, the maximum absolute brightness value in the residual map, the clean beam minor and major axes FWHM and position angle, an estimate of the residual rms phase calibration error, and a file with the flux density and position of each of the image CLEAN components. A comprehensive description of these image parameters can be found in de Witt et al. (2023b).

It is well-established that source structure and its variability can introduce significant errors in astrometric VLBI delay measurements and destabilize source positions (e.g., Charlot, 1990). While sources at K-band generally appear more compact than they do at S- and X-band as demonstrated by recent near-simultaneous S- (2.3 GHz), X- (8.4 GHz), K- (24 GHz), and Q-band (43 GHz) VLBA images (de Witt et al., 2022), they can still exhibit measurable extended emission (see Figure 3). We have therefore embarked on a project to apply source structure corrections directly to our K-band data during the astrometric analysis process, using updated source models obtained from our dedicated K-CRF observing campaigns on the VLBA (e.g., de Witt et al., 2023b).

## 3 Modelfitting

Source characteristics are estimated by fitting models directly to the visibility data through least squares. We use the MODELFIT task within DIFMAP to fit a model consisting of two circular Gaussian components to the calibrated visibilities. This process allows us to determine the flux density and FWHM angular size of the brightest and second brightest components, as well as the vector offset between the two components. To efficiently handle the substantial volume of data, we have developed an automated pipeline dedicated to modelfitting.

In addition to the modelfitting in DIFMAP, we also fit a line through the locations of image CLEAN components using a custom Python routine. This approach provides an effective means of gauging the source's angle of elongation and validating the robustness of the modelfitting in DIFMAP. Both unweighted and flux-density-weighted fits are performed. The outcomes of our modelfitting for the source NRAO140 (J0336+3218) from VLBA observations on 27 Oct 2018 are shown in Figure 4. More detailed information about the modelfitting process is available in de Witt et al. (2023b).

## 4 Structure Quantities and Source Variability

For a source to be considered a suitable VLBI calibrator or reference source, it should ideally be bright and compact at the frequency of observation and exhibit minimal variation over time. To assess source suitabil-

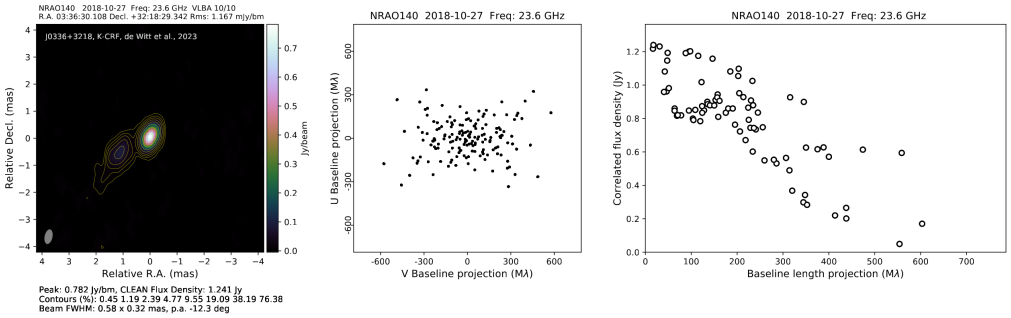


Fig. 1 Example plots for NRAO140 (J0336+3218). Left: image with both contours and colour scale showing brightness. The contour levels are listed below the image, and start at $3\times$ the background rms brightness level and increase by factors of 2 thereafter. Center: the $u, v$-coverage plot. Right: the scan-averaged visibility amplitudes plotted against the baseline length.

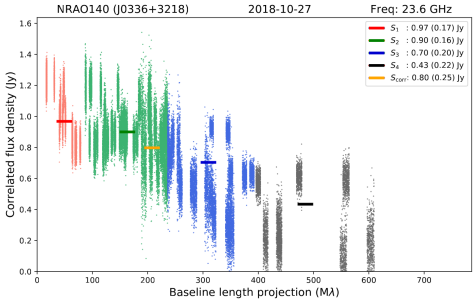


Fig. 2 The correlated visibility amplitude versus baseline length plot for the source NRAO140 (J0336+3218) from 27 Oct 2018. The colours indicate the correlated visibility amplitude and corresponding weighted average over baseline lengths $< 1000$ km (shown in red), between 1000 and $< 3000$ km (shown in green), between 3000 and $< 5000$ km (shown in blue), and 5000 km or more (shown in black). Also shown is the weighted average over all baselines (in orange). For each, the weighted average value is presented alongside the corresponding standard deviation in parentheses.

ity, we utilize the parameters and CLEAN component models derived from our VLBA images. These assessments include the analysis of flux density variability, source structure quantities and their variability, and image quality.

Source structure quantities comprise (1) a measure of source compactness or core domination, (2) radial extent, indicating the extent of source structure and overall angular size, and (3) a structure index ($SI$) quantifying the astrometric quality of a source, defined as $SI = 1 + 2 \times \log_{10}(\tau_{\rm median})$, where $\tau_{\rm median}$ represents the median value of the structure delay corrections, i.e. the additional phase terms due to source structure computed for each CLEAN component and each VLBI baseline for a particular image, in units of picoseconds (ps). An $SI$ value between 0 and 2 indicates compact structure or faint extended emission, while values closer to 3 imply more substantial structural features and values of 4 or more signify pronounced extended emission or intricate structural elements. More detailed information about the structure metrics is available from de Witt et al. (2023b).

Time-series plots of fluctuations in peak brightness, core flux density, CLEAN flux density, and weighted average correlated flux densities for the source NRAO140 (J0336+3218), across 73 distinct epochs of VLBA observations conducted between July 2015 and January 2023, are shown in Figure 5. Time-series plots of the structure metrics, including source compactness, flux-density-weighted radial extent, and SI, for the source NRAO140 (J0336+3218), are shown in Figure 6. These plots reveal trends for this source such as increasing flux density over time, accompanied by a transition toward slightly more core domination. The images themselves show a fading of weak extended emission as the flux density increases.

## 5 Conclusions and outlook

We are actively working on numerous initiatives to enhance, maintain, and refine the K-CRF. Our roadmap includes completing the imaging of all VLBA astrometric K-band sessions from 2019 onwards and characterizing source structures and their temporal variations. Our primary goal is to maintain a dynamic database of high-resolution, multi-epoch K-band images, allowing us to evaluate source strength and morphology contin-

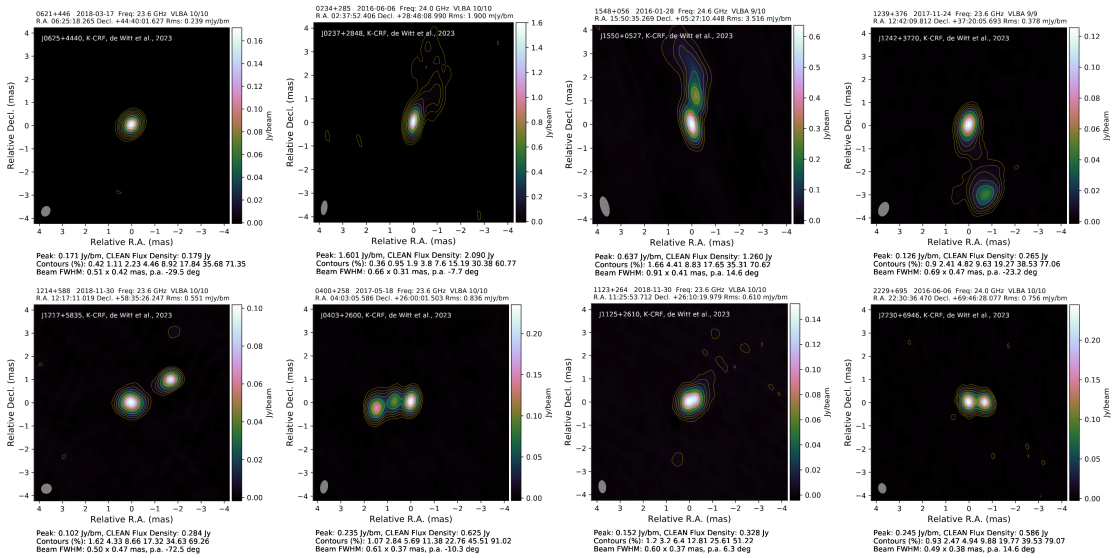


Fig. 3 Images for a selection of K-CRF sources. Both the colour scale and contours show brightness. For each image the colour scale is given at right, and the contour levels listed below. Our images show that the majority of K-CRF sources have a compact structure with no or weak extended emission, similar to that of the first two sources in the top panel. However, some sources do show significant structural features, such as bright extended emission, bright secondary components, or a more complex structure, such as those shown in the remaining six images.

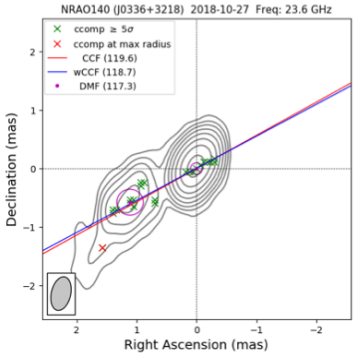


Fig. 4 Contour image of the source NRAO140 (J0336+3218) from 27 Oct 2018. The contours are in grey. The locations of the CLEAN components, ccomp, are shown with green crosses except for the component farthest from the phase centre which is indicated with a red cross. The diagonal red and blue lines are those fitted through the ccomp locations, measuring the overall orientation of the source, with CCF, in blue, being the unweighted fit and wCCF the flux-density weighted one. The position angles of these lines in degrees N through E are given in the legend. Finally, the positions and sizes of the DIFMAP modelfit components (DMF) are shown using magenta circles, also with the position angle in parentheses in the legend.

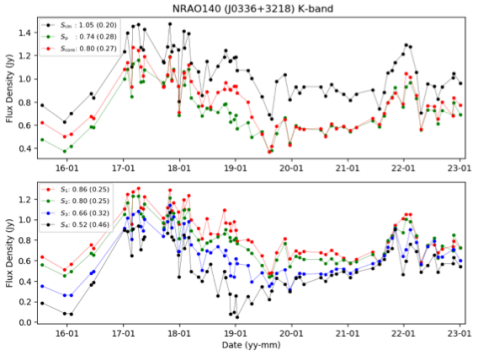


Fig. 5 Time-series plots of the source NRAO140 (J0336+3218) across 73 distinct epochs of VLBA observations between July 2015 and January 2023. The top panel shows the peak brightness, $S_{\rm p}$, core flux density, $S_{\rm core}$, and CLEAN flux density, $S_{\rm cln}$. The bottom panel shows the weighted average correlated flux density for each of the baseline length ranges shown in Figure 2. The corresponding mean value for each quantity, followed by the corresponding variability index in parentheses, are given in the Figure legends at top left in each panel

uously. Our objective is to study the impact of source structure on the K-CRF by modelling the structure effects in our astrometric and geodetic analyses. The outline of our plan is to:

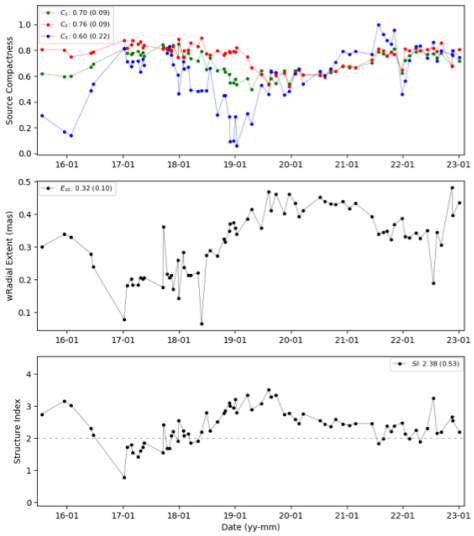


Fig. 6 Time-series plots of the source NRAO140 (J0336+3218) across 73 distinct epochs of VLBA observations between July 2015 and January 2023. These plots show the evolution of source structure metrics over time. The top plot shows the source compactness measures, where $C_1 = S_{\rm p}/S_{\rm cln}$, $C_2 = S_{\rm core}/S_{\rm cln}$, and $C_3 = S_4/S_1$. The middle plot shows the flux-density weighted radial extent, $E_{10}$, in units of mas. The bottom plot shows the structure index, $SI$. In each plot, the mean values for each line, followed by the corresponding standard deviations in parentheses, are given in the plot legends.

1. Quantify the structure and variability of all K-CRF sources.
2. Assess the impact of source structure on the K-CRF.
3. Implement a model to correct for source structure in the astrometric and geodetic analysis software VieVS (Böhm et al., 2018).

The ultimate aim is to produce a CRF with structure corrections applied to all sessions, which would be a significant achievement in the field of absolute astrometry!

## Acknowledgements

 This research was carried out in part at the Jet Propulsion Laboratory, California Institute of Technology, under a contract with the National Aeronautics and Space Administration (80NM0018D0004). The VLBA is managed by NRAO, funded by the National Science Foundation, and operated under cooperative agreement by Associated Universities. The authors gratefully acknowledge use of the VLBA under the USNO's time allocation. This work supports USNO's ongoing research into the celestial reference frame and geodesy. This work was supported by the South African Radio Astronomy Observatory (SARAO,) a facility of the National Research Foundation (NRF) of South Africa.

## References

Böhm J., et al. (2018) Vienna VLBI and Satellite Software (VieVS) for Geodesy and Astrometry. *PASP*, 130, 986, 044503.

Charlot P. (1990) Radio-Source Structure in Astrometric and Geodetic Very Long Baseline Interferometry. *Astron. J*, 99, 1309–1326.

Charlot P., et al. (2020) The third realization of the International Celestial Reference Frame. *A&A*, 644, A159.

de Witt A., et al. (2022) Multi-Frequency Imaging Results of 453 Extragalactic ICRF-3 Radio Sources. *15th EVN Symposium & Users Meeting*, 11-15 July 2022, Cork, Ireland.

de Witt A. (2023) The Growing Potential for K-band (24 GHz) Geodesy. *GGOS Days 2023*, 20-23 September 2023, Yebes, Spain.

de Witt A., et al. (2023b) The Celestial Reference Frame at K Band: Imaging. I. *AJ*, 165, 4, 139.

Greisen S. W. (2003) AIPS, the VLA, and the VLBA. *Information Handling in Astronomy - Historical Vistas*, 285, 109–125.

Napier P. J. (1995) VLBA Design. *Astronomical Society of the Pacific Conference Series*, 82, 59.

Shepherd M. C. (1997) Difmap: an Interactive Program for Synthesis Imaging. *Astronomical Data Analysis Software and Systems VI*, 125, 77.